

## A Review of the Loading Sequence Effects on the Fatigue Life Behaviour of Metallic Materials

K.A. Zakaria<sup>1,2,\*</sup>, S. Abdullah<sup>2</sup> and M.J. Ghazali<sup>2</sup>

<sup>1</sup>Department of Structure and Materials, Faculty of Mechanical Engineering, Universiti Teknikal Malaysia Melaka, Hang Tuah Jaya, 76100 Durian Tunggal, Melaka, MALAYSIA

<sup>2</sup>Department of Mechanical and Materials Engineering, Universiti Kebangsaan Malaysia, 43600 UKM Bangi, Selangor, MALAYSIA.

Received 21 October 2016; Accepted 28 November 2016

### Abstract

This paper reviews the previous literature on the effects of loading sequence on fatigue life behaviour. Through load interaction, load sequences can significantly affect fatigue life. The study on fatigue life under spectrum loading sequence is complex because it involves many interaction parameters. Therefore, the experimental and simulation findings of previous studies focusing on load sequence effects on fatigue life assessment are worthy of a review. The content of this review leads to a better understanding of the loading sequence effects on the fatigue life assessment and other possible interaction involvement.

*Keywords:* Fatigue life, Load sequence effect, Spectrum loadings

### 1. Introduction

Engineering components involved in movement mechanisms are commonly subjected to cyclic or fluctuating stress during service. Relevant cases often refer to the field of automotive study, such as an automobile axle that experiences many repetitions or reversals of applied stress during the service life of the vehicle. Other examples are bent and released leaf springs or most aircraft parts that are subjected to repeated loads during its take-off and landing. Various parts of moving machines also undergo severe vibration with load fluctuations.

Fatigue failure occurs under cyclic or fluctuating loading [1,2]. Structural or engineering components are prone to fatigue when subjected to a certain number of cyclic loading [3], which normally occurs below the ultimate strength of a material. Fatigue also usually occurs without warning after a progressive degradation of the material subjected to cyclic loadings [4,5]. Fatigue is recognised as one of the major failure mechanisms in structural and engineering components, accounting for about 90% of all mechanical failures [6-8]. Fatigue failure may ensue in a wide range of application, from simple objects to complex structures such as automotive, marine, and aircraft components. Therefore, the fatigue life assessment of engineering applications is highly important [9].

Many factors affect the fatigue life of structural and engineering components, including geometric models [10], microstructures and grain sizes [11,12], surface finish through modelling works [13] and experimental findings [14,15], loading conditions related to both constant and variable amplitudes [16-19], environment through corrosion [20], and temperature [21-23]. Based on the related content described in [16-19], load sequence effects are important

factors to consider in assessing the fatigue life of metallic materials. Considering the effect of load interactions in spectrum loading contributes to higher accuracy of fatigue life prediction, whereas disregarding the effect of load interaction in fatigue calculation under the variable amplitude loading (VAL) can lead to completely invalid life predictions.

Therefore, this comprehensive review examines the loading sequence effects under various parameters and loading variables, and highlights their advantages and disadvantage to the total life of the components. The factors that contribute to the number of fatigue life cycles require deeper understanding. Furthermore, as loading sequences are mostly performed at room temperature, understanding their effects at normal conditions may reveal other factors that contribute to fatigue life, such as temperature and environmental effects.

### 2. Brief Overview of Fatigue Life Assessment

Fatigue life usually refers to the number of stress or strain cycles structures and components can withstand before failure. Fatigue life assessment determines the life of components that are subjected to certain loading conditions. Fatigue life can be determined from experimental works, with the formulation or simulation obtained using certain software [3]. In the design stage, an exhaustive understanding of material behaviour is critical to preserve the safety and integrity of the component. The service lifetime of the component can be estimated from the number of loading cycles before cracks form. The fatigue crack growth (FCG) rates are the main parameters that require consideration [24]. Total fatigue life is a combination of the number of cycles before cracks form and propagates until the final failures.

Three basic approaches are commonly used for fatigue damage calculations: stress-life approach, strain-life

\* E-mail address: kamarul@utem.edu.my

approach, and crack propagation method. The stress-life approach has been used as a standard method for fatigue life assessment since the 1800s. This method uses cyclic stress as a control variable, which is distinguished from other types of fatigue analysis. Stress-life analysis is suitable for high-cycle fatigue that involves little plastic deformation due to cyclic loading. The strain-life approach is advantageous for the analysis of fatigue life subjected to the VAL, in which the load sequence effect is essential. This approach considers both elastic and plastic strain behaviour of the material. In contrast to stress-life and strain-life approaches to fatigue, fracture mechanics assumes cracks to exist in materials and structures. The crack propagation approach is based on the stress intensity factor range [25].

In general, the stress-life approach is directly related to the service load to ensure safe operating life based on a linear presentation of cumulative damage [26]. The stress-life (*S-N*) curve is useful for estimating the fatigue life by providing the number of cycles as failure data at certain levels of applied stress. The *S-N* curve is usually plotted on a semi-log or log-log scale that contains experimental data of a constant amplitude loading (CAL). Fatigue data are obtained by testing a smooth specimen often performed at zero mean stress.

In the experimental fatigue life assessment, the basic concept is based on the number of cycles to failure. The *S-N* curve is developed by using tabular data that follow the Basquin equation [10], which is written as follows:

$$\frac{\sigma}{2} = \sigma_a = \sigma_f'(2N)^{b'} \tag{1}$$

where  $\sigma_a$  is the stress amplitude,  $\sigma_f'$  is the fatigue strength coefficient,  $2N_f'$  is the number of reversals, and  $b$  is the Basquin exponent. Fig.1 indicates a typical example of the *S-N* curve of aluminium alloy, AA6061, obtained from the experimental data test [2].

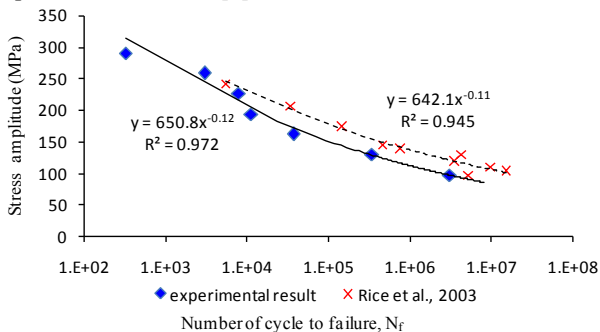


Fig. 1. Normal *S-N* curve of AA6061 tested at room temperature [2]

The *S-N* curve is developed based on a constant stress range  $\sigma_r$ , or constant stress amplitude  $\sigma_{an}$  applied on the specimen until final failure. The mean stress  $\sigma_m$  can significantly influence the fatigue life of the material. Fig. 2 shows a typical fatigue life behaviour subjected to different mean stress loadings. Fatigue strength of a material decreases significantly as the tensile mean stress increases but increases as compressive mean stress increases [28, 29].

Fatigue data at any endurance can be cross-plotted to demonstrate the effect of mean stress on fatigue strength at the chosen endurance. At mean stress equal to the ultimate strength of a material, the allowable stress amplitude is suggested to be zero as the material is at the breaking point. Therefore, the stress effect can be analytically defined by the

modified Goodman and Gerber equations, which are given in Equations (2) and (3), respectively [3,26]:

$$\frac{\sigma_a}{S_e} + \frac{\sigma_m}{S_u} = 1, \tag{2}$$

$$\frac{\sigma_a}{S_e} + \left(\frac{\sigma_m}{S_u}\right)^2 = 1, \tag{3}$$

where  $\sigma_a$  is the stress amplitude,  $S_e$  is the stress amplitude at zero mean stress,  $\sigma_m$  is the mean stress, and  $S_u$  is the ultimate tensile strength. Fig. 3 illustrates these two equations on fatigue design. Therefore, the mean stress requires consideration in predicting the fatigue life of components, especially those subjected to VAL, as it has a noticeable impact on fatigue life behaviour.

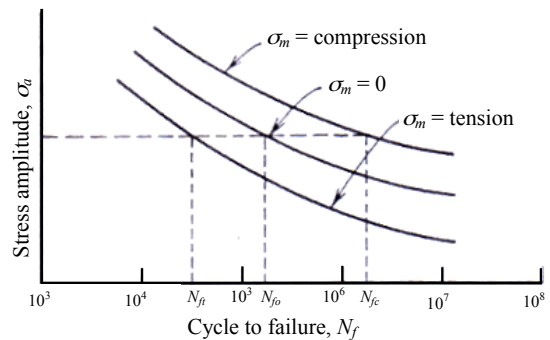


Fig.2. Fatigue life behaviour under different mean stress [3]

In VAL, the interaction of loading in cycles causes localised stress and strain. The relation between stress  $\sigma$  and strain  $\epsilon$  in cyclic loadings is often represented by the Ramberg-Osgood equation:

$$\epsilon = \frac{\sigma}{E} + \left(\frac{\sigma}{K}\right)^{\frac{1}{n}}, \tag{4}$$

where  $E$  is the modulus of elasticity,  $K$  is the strain hardening coefficient, and  $n$  is the strain hardening exponent.

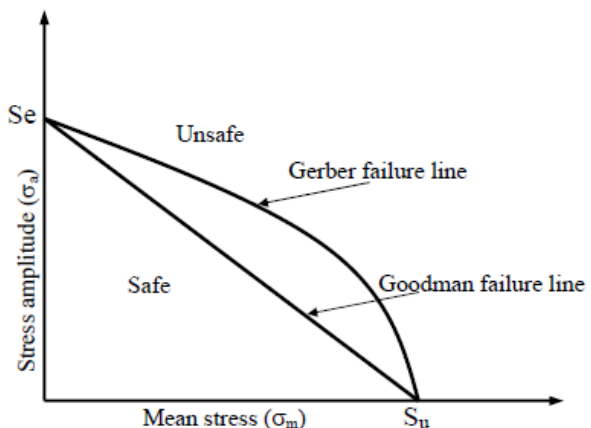


Fig. 3. Schematic of the Goodman and Gerber mean stress correction [26]

The strain-life approach is meant to be used in analysing the localised fatigue cracks based on the occurrence of crack initiation. It is suitable for applications of small component

design that usually involves localised stress and strain subjected to low cycle fatigue loadings. The method is also intended to examine the failure of ductile materials with a relatively short fatigue life and when low plasticity occurs with long fatigue life. Therefore, this approach is a comprehensive one that can be used in lieu of the stress-based method [30].

The application of strain-life analysis requires a description of the material response to cyclic elastic-plastic strains as well as of the relationship between these strains and fatigue life with crack initiation. The basic strain-life relationship is based on the Coffin–Manson and Basquin relationship. In 1910, Basquin proposed a linear relationship between stress amplitude and endurance, as stated in the Basquin formulation referred to in Equation (4). Moreover, Coffin and Manson obtained the relationship between the number of cycles to failure and strain amplitude in 1954, as represented by Equation (6) [31]:

$$\sigma_a = \sigma'_f (2N_f)^b \tag{5}$$

$$\epsilon_a = \epsilon'_f (2N_f)^c \tag{6}$$

Therefore, the combination concept between the Basquin approach and the Coffin–Manson relationship is based on the total strain amplitude, which is written as follows:

$$\epsilon_a = \frac{\sigma'_f}{E} (2N_f)^b + \epsilon'_f (2N_f)^c, \tag{7}$$

where  $\epsilon_a$  is the true strain amplitude,  $\sigma'_f$  is the fatigue strength coefficient,  $b$  is the fatigue strength exponent,  $\epsilon'_f$  is the fatigue ductility coefficient,  $c$  is the fatigue ductility exponent,  $E$  is the modulus of elasticity, and  $2N_f$  is the number of reversals to failure for a particular stress range. Fig. 4 exhibits the strain-life curve obtained from the superposition of the elastic and plastic strain amplitude.

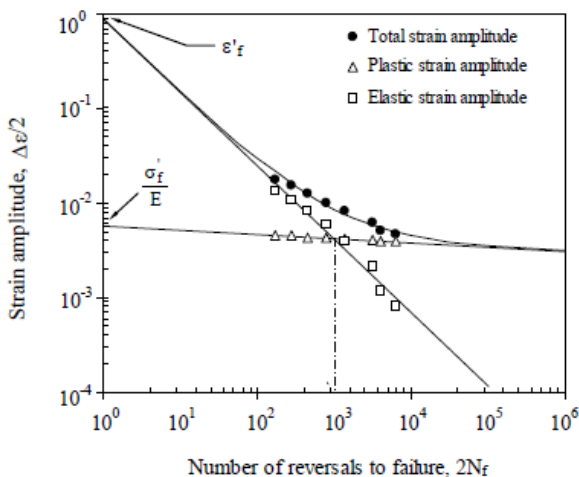


Fig. 4. Typical example of a strain-life relationship for material aluminium alloy 6061-T651 [31]

Non-zero mean stress significantly influences the fatigue life of materials because the tensile or compressive mean stress can lead to acceleration or retardation of FCG. By considering the mean stress effect, two other strain-life models were expanded from the equation (3), namely, the Morrow strain-life model and the Smith-Watson-Topper

(SWT) [32]. In the Morrow strain-life model, a relationship between strain amplitude and fatigue life is represented by the following equation:

$$\epsilon_a = \frac{(\sigma'_f - \sigma_m)}{E} (2N_f)^b + \epsilon'_f (2N_f)^c. \tag{8}$$

The SWT strain-life model is represented by the following equation:

$$\epsilon_a \sigma_{max} = \frac{(\sigma'_f)^2}{E} (2N_f)^{2b} + \sigma'_f \epsilon'_f (2N_f)^{b+c}, \tag{9}$$

where  $\sigma_m$  is the mean stress and  $\sigma_{max}$  is the maximum stress in cycles.

Fatigue failures of structures and components occur under cyclic loadings even if the maximum value of the cyclic load is much lower than the static strength of the material. The fatigue damage for one cycle can be calculated as

$$D = \frac{1}{N_f} \tag{10}$$

Fatigue damage increases with the applied loading cycles in both CAL and VAL. However, the characteristics of damage accumulation under different loadings are different. Among all the fatigue damage accumulation rules, the linear damage accumulation known as the Palmgren-Miner's rule is probably the most commonly used because of its simplicity [17, 33-34]. The Palmgren-Miner's rule is expressed in fatigue damage accumulation as

$$D = \frac{n_1}{N_1} + \frac{n_2}{N_2} + \frac{n_3}{N_3} + \dots + \frac{n_i}{N_i} = \sum_{i=1}^k \frac{n_i}{N_i} \tag{11}$$

where  $D$  is the fatigue damage of the material,  $n_i$  is the number of applied loading cycles corresponding to the  $i$ th load level, and  $N_i$  is the number of cycles to failure for the  $i$ th load level from constant amplitude experiments. The Palmgren-Miner's rule suggests that any structure with  $\Sigma(n/N) < 1$  is safe for operation. However, its major limitation is the lack of consideration on the load sequence effect, that is, the interaction between higher and lower stress levels. Therefore, depending on load history, the Palmgren-Miner's rule may under- or over estimate fatigue damage [34,35].

A non-linear model was proposed by Marco and Starkey, who suggested the replacement of the Palmgren-Miner's rule with the following equation [35]:

$$D = \left(\frac{n}{N}\right)^\alpha \tag{12}$$

where  $\alpha$  is a function of the applied load to be identified based on the experimental data. The load dependency of  $\alpha$  enables the description of the load sequential effects.

The fundamental FCG behaviour obtained under the CAL can be plotted on the log-log of  $da/dN$  versus  $\Delta K$ . The plot has a sigmoidal shape that can be divided into three major regions [37], as shown in Fig. 3. Region I is near the threshold and indicates the threshold value,  $\Delta K_{th}$ , below which FCG is not observed. This threshold occurs at FCG

rates in the order of  $1 \times 10^{-10}$  m/cycle or less. Below  $\Delta K_{th}$ , fatigue cracks are characterised as non-propagating cracks. Region II essentially indicates a linear relationship between  $\log da/dN$  and  $\log \Delta K$ , which correspond to the formula

$$\frac{da}{dN} = A(\Delta K)^n \quad (13)$$

Equation (12) is known as the Paris equation, where  $n$  is the slope of the line, and  $A$  is the coefficient found by extending the straight line to  $\Delta K=1 \text{ MP}\sqrt{\text{m}}$ . In region III, FCG rates increase as they approach instability, and little FCG life is involved.

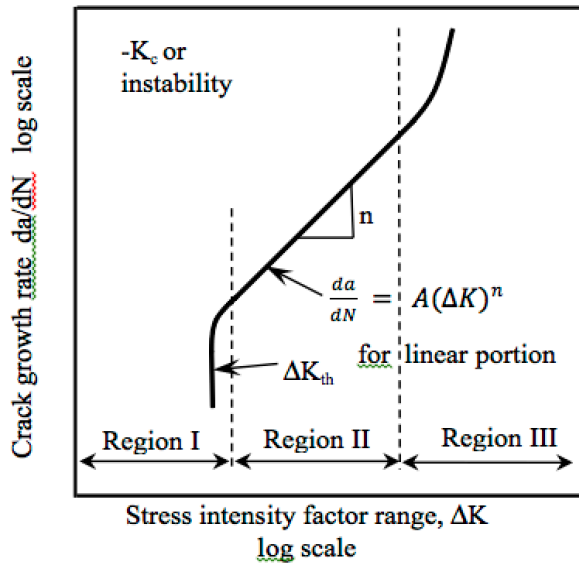


Fig. 5. Typical characteristic of the FCG curve [36]

In VAL conditions, the variability in stress amplitude, mean stress, stress ratio, position, and magnitude of overloads and underloads affect the FCG rates. Tensile overload in loading sequences causes FCG retardation [37-39]. A compressive underload accelerates the crack propagation rates [40, 41]. In the case of a compressive underload that immediately follows a tensile overload, the amount of retardation is reduced. Conversely, a compressive underload applied prior to overloading produces only small changes in the amount of crack retardation.

Beden et al. [37] extensively simulated the load sequence effects in block loadings designed at various mean stresses using various FCG models. Fig. 6 demonstrates that the FCG rates of aluminium alloy are significantly affected by the load sequence. The acceleration or deceleration of the overall FCG depends on the overloading frequency. Therefore, the load sequence effect on FCG rates highly depend on the interaction of overloads and underloads in sequence, subjecting the fatigue life assessment to VAL more complex than CAL.

### 3. Effects of a Single Overload in a Loading Sequence

Load variability represents a characteristic feature of the real load spectra. The two types of variability in the load spectra are the distribution of the loading amplitude and mean stress level of the fatigue cycles, and the distribution versus time for a given load level [42]. The relative position of cycles

within a spectrum can significantly modify the fatigue life of a component. For instance, overloading in loading sequences can cause crack retardation and delayed FCG rates.

An overload is a cyclic loading with higher amplitude compared with background cycles in a sequence. Overload normally occurs either at the beginning, middle, or end of the loading sequence and may proceed once or multiple times in the sequence. The effects of overload on fatigue life determination have been extensively studied [38-39, 43] because this loading type can lead to significant load interaction effects. Moreover, this loading pattern can represent critical measured loading that exhibits variable forms [44, 45]. Therefore, reviewing the effects of overloading on fatigue life, which consist of sequence loadings such as the effect of single overload, multiple overloads, overload wave types, and overload location, among others, is important.

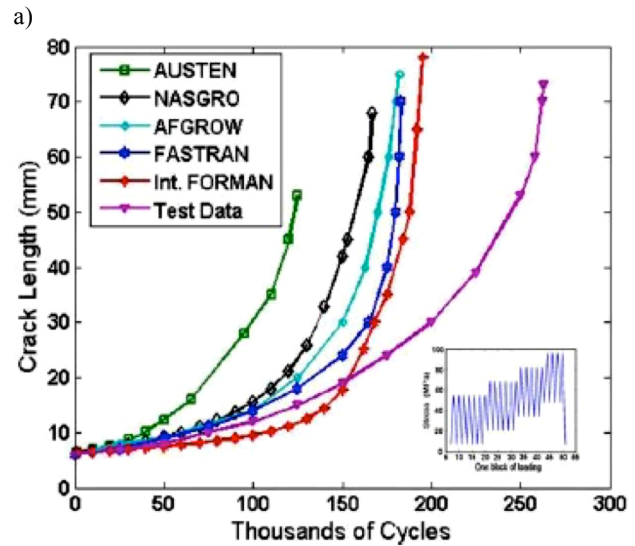
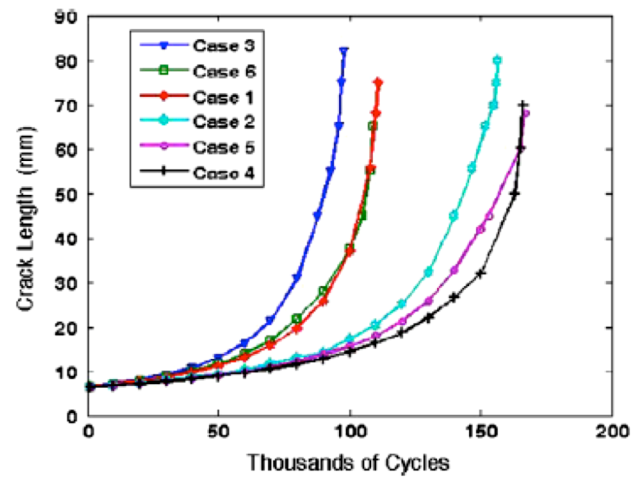


Fig. 6. FCG behaviour subjected to (a) different loadings sequences and (b) different FCG models [37]

Ray and Patanker [38] observed the FCG behaviour under CAL and a single overload, with the loading pattern shown in Fig. 7. The cyclic load was in the tension-tension condition with a stress range of 98 MPa to 147 MPa. An overload of 196 MPa was then introduced when the crack length reached 15 mm. In response to an overload excitation in the sequence, the FCG rates suddenly increased and then subsequently decreased to their minimum values, followed

by a gradual approach to the level of the baseline steady-state, as shown in Fig. 8. Therefore, FCG was retarded because of the fast rise and subsequent slow decay of stress opening.

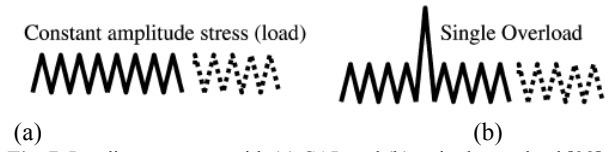


Fig. 7. Loading sequence with (a) CAL and (b) a single overload [38]

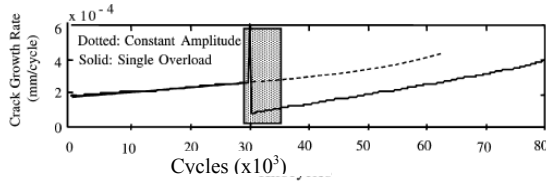


Fig. 8. Overload response of a typical FCG process [38]

Generally, the two types of crack retardation models are based on the plastic ahead crack tip and the crack closure concepts [38, 43]. Based on the plastic ahead crack tip, the plastic zone size is relatively small when subjected to CAL, as indicated by the black oval in Fig. 9. This plastic zone can be assumed as a material resistant to the FCG process. After a single overload applied on the loading sequence, the resulting plastic zone enlarges, as indicated by the grey colour. Consequently, FCG passes through a larger plastic zone, which is severely retarded because of the material's increased resistance to FCG. Once the crack expands out of the overload plastic zone, normal FCG rates prevail upon reaching the plastic zone of the original size, as indicated by the oval.

For the crack closure concept, overloading sequences with respect to CAL produce large compressive stresses at the crack tip, resulting in crack closure. Consequently, a large portion of tensile overload is used to 'open' the crack, dominating the much smaller effective load and FCG retardation. The range of applied stress effectively reduces the FCG with the formation of crack closure. Furthermore, the crack opening stress that relates to the magnitude of stress necessary to fully open the crack depends on the previous load history. When the FCG passes through the overload plastic zone, the residual stress in the zone increases the load required to open the crack, thus causing FCG retardation. Therefore, crack closure models determine the required opening stress throughout the load history [37, 43].

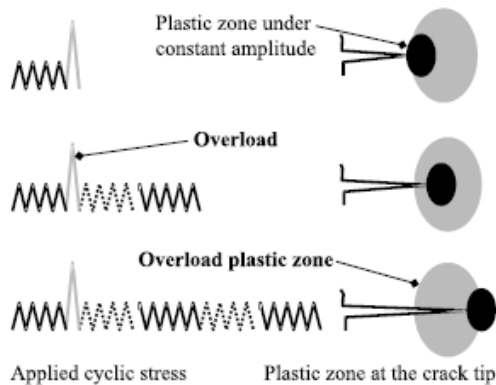


Fig. 9. Influence of fatigue overload on the plastic zone size [38]

The crack closure measurements indicate that FCG rates following an overload are related to the extent of crack closure resulting from the overload. The overload percentage [46] is defined as follows:

$$\text{Overload percentage} = \frac{K_{max\,OL} - K_{max\,b}}{\Delta K_{max\,b}} \times 100, \quad (14)$$

where  $K_{max}$  and  $\Delta K$  are the maximum stress intensity factor and stress intensity factor range, respectively. The subscripts  $OL$  and  $b$  refer to the overload and baseline levels of cycling, respectively. This overload percentage represents the VAL trend in the cycles and directly influences the loading sequence effect.

In a similar study, Ishihara et al. [46] used a compact tension (CT) specimen with 6mm thickness and made of an aluminium alloy AA6061-T6. During the test, the specimen was subjected to 100% to 300% overloads at average stress ratio, with  $R$  from 0.1 to 0.9. Fig. 10 plots the summary of the experimental number of delay cycles  $N_d$  at overload levels of 100%, 200%, and 300% as a function of stress ratio. The number of delay cycles  $N_d$  significantly increased with the overload percentage, clearly indicating that the crack retardation process is significantly influenced by the overload percentage. Finally, the presence of overloading in a sequence reduced fatigue life accordingly.

Harmain [47] performed a computational technique to simulate the effect of overload ratio on FCG rates. A single overload was introduced with three different overload ratios of 2.50, 2.25, and 2.00. Fig. 11 presents the results accomplished by using the concept of plasticity zone interaction and the FCG related findings. Triangular spike dips for FCG rates are demonstrated from the computational analysis. The application of the overload retarded the FCG rates from the baseline value of CAL. Fig. 11 illustrates that the lowest FCG rate was attained at the highest overload ratio of 2.50, for which the retardation effect increased with the overload ratio.

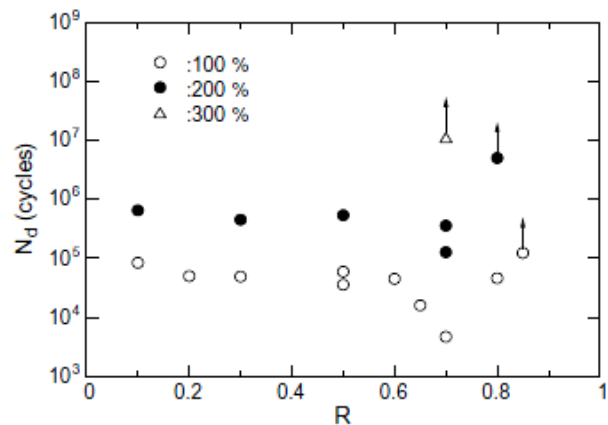


Fig. 10. Comparison of delay cycles subjected to certain overload percentages throughout different stress ratios [46]

The phenomenon of reduced or arrested FCG rates after experiencing overloads can also be explained by the crack opening ratio  $U$  [48]. In overloading, the increase in maximum stress  $\sigma_{max}$  with unchanged minimum stress  $\sigma_{min}$  leads to the decrease in stress ratio,  $R$ , where

$$\text{Stress ratio, } R = \frac{\sigma_{min}}{\sigma_{max}} \quad (15)$$

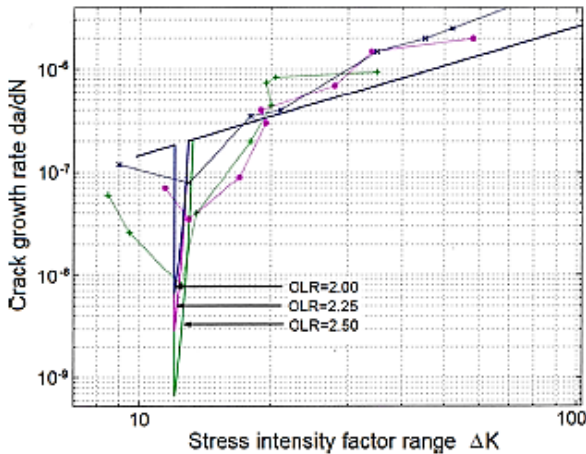


Fig. 11. FCG rates with respect to stress intensity factor range for different overload ratios [47]

Therefore, the decreasing stress ratio causes the same reduction in the crack opening. In unloading, stress ratio similarly changes as the crack opening widens.

In another work, overload waveforms influence the retardation of FCG rates. Fang et al. [49] investigated the effect of overloading using both sinusoidal and trapezoid waveforms, as presented in Fig. 12. They concluded that the overload ratio produced a significant impact and that the overload waveform also contributed, with a slight effect on FCG rates. Compared with the sinusoidal overload waveform, the trapezoidal overload waveform caused slightly longer delay of FCG in polycarbonate and acrylonitrile-butadien-styreneor alloys. This finding indicates that the trapezoidal overload waveform contributes as lightly higher retardation effect than the sinusoidal overload waveform. The trapezoidal waveform holds a slightly longer time overload that leads to a slightly larger plastic zone at the crack tip.

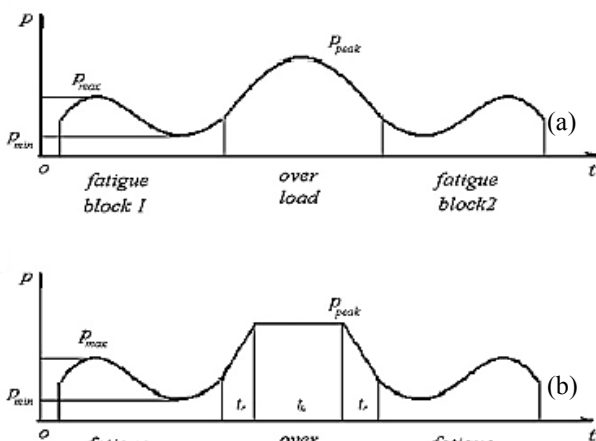


Fig. 12. Fatigue overload patterns: (a) sinusoidal waveform, and (b) trapezoid waveform [49]

#### 4. Effect of Multiple Overloads and Underloads on the Sequence

Multiple overloads in the sequence can also influence the retardation effects associated with fatigue failure. Borrego et al. [39] studied the effect of overload spacing on the FCG rates of Middle-Tension M(T) specimens made of aluminium alloy Al 6082-T6. Fig. 13 shows the effect of periodically applied overloads for the number of baseline cycles between overloads,  $n_{BL}$ . A re-application of an overload from the baseline cycle leads to the retardation of FCG rates. Nevertheless, when the overload is reapplied in phases of descending FCG rates, the retardation effect is reduced as it disrupts the crack retardation process induced by the preceding overload. Therefore, overload intervals must be sufficiently long to obtain the most effective FCG retardation effects.

Daneshpour et al. [43] used a centre-crack specimen made of aluminium alloy Al 2139-T8 to study the effect of single and multiple overloads on FCG rates. A single overload level of 136 MPa was applied within the CAL, and multiple overloading tests were conducted with periodic 1000 cycles between each overload. A single overload extends the fatigue life of the Al 2139-T8 base metal specimens by approximately 5% and that of the welded panels by approximately 80%. Multiple overloads extend the fatigue life in the base metal by approximately 480% and that of the fatigue life for weld joints at approximately 230%. Fig. 14 presents the distribution of the corresponding fatigue lives. Therefore, the effect of multiple overloads on the crack retardation in welded specimen is not as significant as that on the base metal. Other studies [50-52] suggest that a closely applied multiple overload may interact among each other, thus influencing the overall retardation effect with either enhanced or reduced FCG. This interaction depends on the magnitude and interval/frequencies of the applied overload.

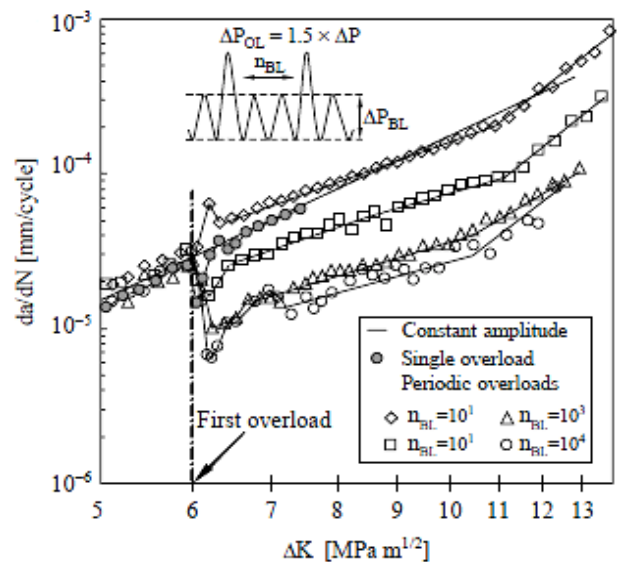


Fig. 13. Effect of the spacing between overloads [39]

Apart from overload, the presence of underload in the sequence produces a different behaviour of the material FCG rates. Zitounis et al. [40] applied a single underload at certain stress ratios in a sequence, as shown in Fig. 15, on a CT specimen made of aluminium alloys AA8090-T852 and AA7010-T76351. Their results indicate that the FCG rates under a loading sequence containing tensile underload accelerates the FCG rates compared with those of CAL. The crack opening stress level is immediately reduced after the

underload application and then gradually increases with the subsequent constant amplitude cycle. After a large number of cycles, the FCG rates reach a steady-state level. Other researchers agree that a compressive underload accelerates the FCG rates relative to the background rates [37, 41].

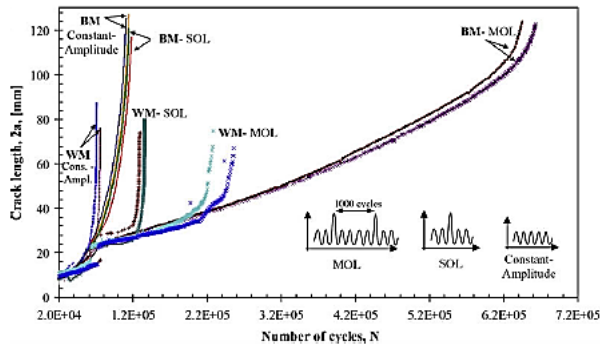


Fig. 14. Experimental results of the fatigue tests of welded and homogeneous specimens of Al 2139-T8 under CAL, single, and multiple overloads [43]

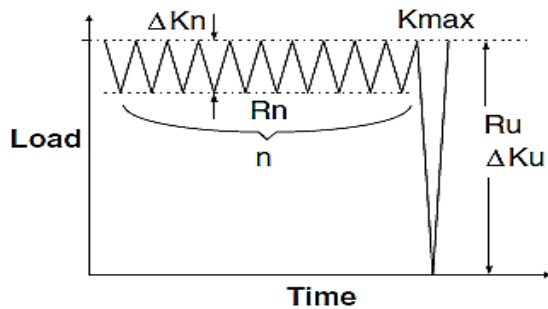


Fig. 15. A typical single overload applied in a sequence loading [40]

Any small cycle below the fatigue limit does not usually damage the materials. However, Varvani-Farahani et al. [53] reported that when tensile, compressive, or single cycle overloads or underloads are periodically inserted within a group of small cycles below the fatigue endurance limit, the small stress cycles following these events significantly contribute to damage accumulation. An overload or underload periodically applied in a small stress cycle background reduces the crack closure stress, thus enhancing the effective crack driving force. The findings are similar to those in [36], indicating that intermittent small cycles with amplitudes as low as 50% on the endurance limit within regular LCF or HCF service loading conditions can be very damaging. These findings caution engineers about indiscriminately ignoring these seemingly harmless cycles from their fatigue life calculations.

Overloads in cycles retard FCG, and underloads accelerate FCG. Silva [54] reported that overload events at a negative stress ratio could accelerate FCG instead of the expected retardation. The size of cyclic plastic zone under negative stress ratio is almost the same as the monotonic condition. An overload in cycles causes increases in both the monotonic plastic and the cyclic plastic areas. As the size of cyclic plastic zone and monotonic is nearly the same, the residual stress shielding effect (compressive residual stresses) is much smaller at a negative stress ratio compared with that at a positive stress ratio. Thus, the effect of reducing the cyclic plastic area is small. During the overload period, the cyclic plastic zone size remains larger than its

size previous to the overload. The overall behaviour of material after the overload consequently accelerates instead of retards the FCG.

### 5. Sequence Effect in the Spectrum Loading

In real applications, most of the components are subject to stress and strain that vary with time. The load pattern with time history is most likely irregular and random in manner. The main problem in analysing this loading type is the identification of the corresponding stress range in the cycle. Therefore, a method of stress cycle count is necessary to be used. Rainflow counting results in closed hysteresis loops that represent a counted cycle [6]. The information of cycle distribution required in fatigue life assessment can be obtained through a rainflow counting of the loading history, as illustrated in Fig. 16. Therefore, rainflow counting is the generally accepted and recommended procedure for the estimation of fatigue life of structures subjected to random loading [33, 55-56].

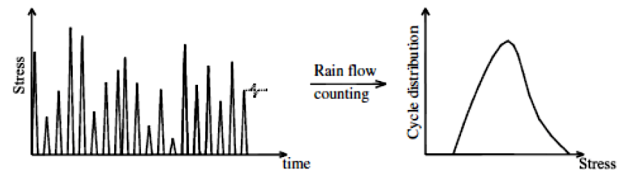


Fig.16. Schematic illustration of cycle distribution using the rainflow counting method [56]

Spectrum loading is widely used in fatigue analysis to study the loading sequence effect in cycles, significantly influencing fatigue life, and is thus important in considering fatigue life assessment [34,37,39,43,64]. Equivalent damage is one of the methods that can be used to construct spectrum loading from the service loads. For example, the flight-by-flight load history (random loading) can be converted to CAL based on the equivalent damage [57]. Pereira et al. [35] used the maximum stress that induces the same damage when applied on the same total number of cycles of block loading. For an automotive application, Abdullah et al. [58] determined good justification in the retention of fatigue damage features while editing fatigue data for accelerated fatigue tests.

Various forms of spectrum loading are introduced into the fatigue life assessment, most of which can be grouped into CAL, high-to-low, and low-to-high sequence loadings [59-61]. Lin et al. [59] studied the fatigue-creep behaviour using different step loading and found that a high-to-low sequence of two-step loading at a constant temperature is more damaging than the corresponding low-to-high sequence. First, the specimen was applied with stress and temperature  $(\sigma_1, T_1)$  for a period of time  $t_1$  and then applied with a second stress and temperature  $(\sigma_2, T_2)$  until failure. In the case of two-step loading at room temperature, a higher crack density was generated at the first-step loading in a high-to-low sequence compared with the low-to-high sequence at the same consumed lifetime ratio. In this regard, the specimens applied with a high-to-low sequence were subjected to the second-step loading at a weaker state compared with the corresponding low-to-high sequence loading. Therefore, a high-to-low sequence loading generates a lower sum of life fraction and shorter fatigue life.

Walter et al. [60] studied the effect of multi-step loading on the total fatigue life of ferretic stainless steel. The experiments used round specimens with 8.8 mm diameter and 20 mm gauge length. The test was performed under strain load control with a stress ratio of -1. Fig.17 indicates the condition of the two-step loading used in the experiment, that is, from high-to-low and low-to-high sequences. Both high-to-low and low-to-high stress levels are applied to study the loading sequence effect on fatigue life. The designed two-load steps indicate a different value of the progression of the maximum stress at a particular step loading.

Fig. 18 presents the evolution of the maximum stress for different load steps. The normalised fatigue life is longer when starting with low rather than high strain amplitude. The material behaviour exhibits strong softening at the beginning of the single step experiment, followed by a continuous linear softening until the initiation of a macro-crack. Increasing the total strain amplitude at the beginning increases the softening potential, thus decreasing the lifetime because of higher stresses and plastic deformations during one cycle. Therefore, changing from high to low load condition usually leads to lower normalised total lifetimes compared with the opposite case. The progression of the damage behaviour directly depends on the softening progression.

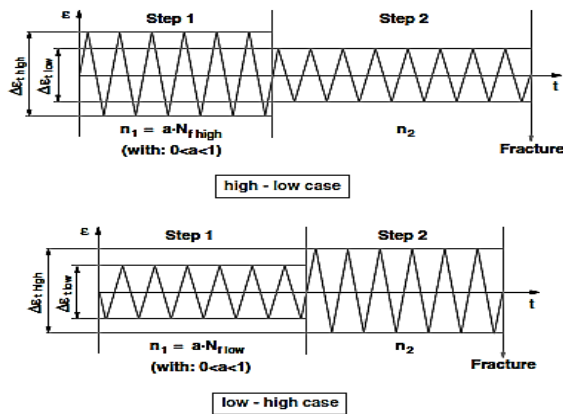


Fig. 17. Two steps of spectrum loading used in the experiment [60]

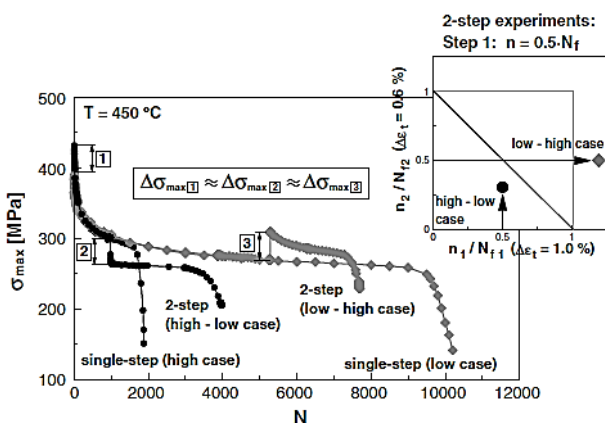


Fig. 18. Comparison between progression maximum stresses for different load conditions [60]

Borrego et al. [61] studied the effect of spectrum loading on FCG rates and reported that the FCG rates under the low-to-high sequence loadings are higher than those under the high-to-low sequence loading. Using the experimental procedure, they investigated the high-to-low and low-to-high

sequences at a stress intensity range of 6, 9, and 12 MPa.m<sup>1/2</sup>. The results in Fig. 19 indicate that a brief initial acceleration of FCG rates immediately followed after the overload. The subsequent FCG rates decreased until their minimum value, followed by a gradual approach to the level of the baseline steady-state. The effect of the high-to-low sequence was determined as similar to the ones observed for a peak overload. In contrast, the low-to-high sequence accelerated the FCG rates above the steady-state level, followed by a gradual reduction to the corresponding steady-state level. The low-to-high sequence loading was applied at a constant minimum stress level, and the values of the mean stress increased from the first to second steps. Fatigue strength decreases as tensile mean stress increases [62, 63].

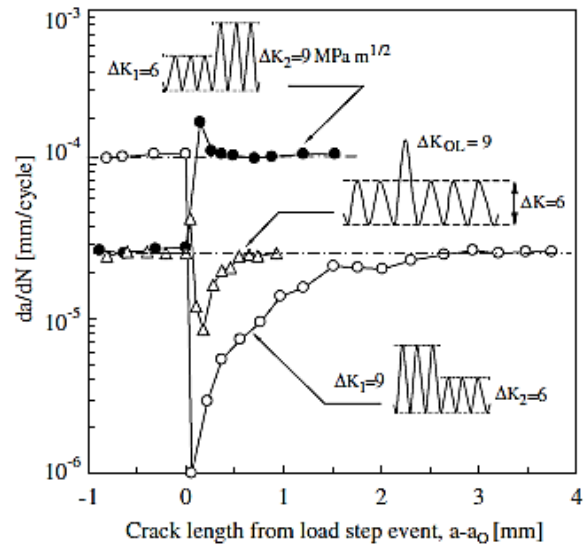


Fig. 19. Transient behaviour following a single tensile overload, high-to-low, and low-to-high sequence loading [61]

The effect of the mean stress in the sequence loading on the fatigue crack opening has been previously discussed. For fatigue design, a compressive mean stress is beneficial, but a tensile mean stress is detrimental. Chu and Chernenkoff [63] used the constant maximum and minimum stress tests to record the mean stress effects on fatigue life. By maintaining  $S_{max}$  at a fixed level in a constant maximum stress test set, the effect of  $S_{max}$  on the opening stress is constant. As a result, the variation of opening stress observed on the tests of different stress amplitudes reveals its dependence on  $S_{min}$ . Similarly, by retaining  $S_{min}$  at a fixed level in the constant minimum stress test set, the variation of opening stress observed on the tests of different stress amplitudes reveals its dependence on  $S_{max}$ . Fig. 20 (a) shows the condition of constant maximum stress and the dependence of crack opening on the minimum stress in the cycles. Fig. 20 (b) presents the condition of the constant minimum stress and the dependence of crack opening on the maximum stress in cycles. Both figures reveal that the fatigue crack opening depends on the mean stress, thus influencing the total fatigue life. As mean stress is common in structures, the capability to accurately predict the effect of mean stress is highly important for the fatigue design of engineering components.

Lee et al. [64] studied the FCG rates using the VAL, with the tension and tension-compression types of load spectra, as shown in Fig. 21. FCG rates were observed to be faster when subjected to tension-compression than when subjected to the tension-type spectrum loading. The reason is

that the tension type spectrum loading contains tensile overloads that retard the FCG rates, whereas the tension-compression type spectrum loading contains underloads that accelerate the FCG rates, as clearly revealed in the findings. The retardation and acceleration effects are considered to be primarily associated with the interaction of overloads and underloads in the spectrum loading.

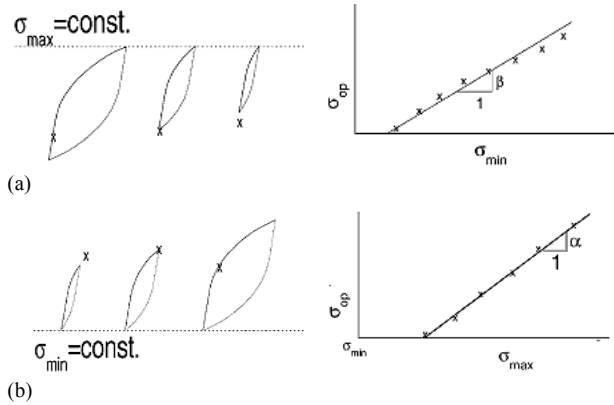


Fig. 20. Crack opening with the corresponding applied stress levels: (a) constant maximum stress and (b) constant minimum stress [63]

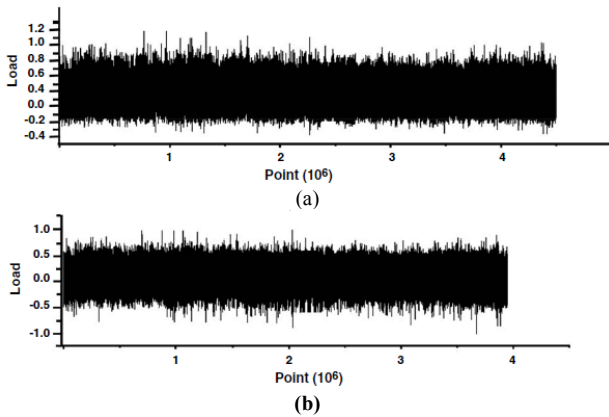


Fig. 21. (a) Tension-type and (b) tension-compression-type load spectrums [64]

The review of the presented previous works clearly indicates that tensile overloads and compressive underloads in loading sequence cause FCG retardation and acceleration, respectively. Overall, the effect of sequence on spectrum loading depends on the arrangement of the loading condition. Furthermore, the experimental results are based on various types of materials used with different magnitudes and positions of the load steps, stress ratio, and mean stress, among others, contributing to the different FCG rates and the total fatigue life of metallic materials.

## 6. Fractography Behaviour under Variable Amplitude Loading

Failure analysis usually correlates the failure of structures with its causes. Fractography techniques using high-magnification microscopes, such as scanning electron microscope (SEM), are extensively used in fatigue studies to identify the modes of failure and correlate them with material behaviour and properties [65,66]. Macroscopic observation on the specimen fatigue fracture surface can clearly distinguish two discrete regions identified between the fatigue and rapid fracture regions [67]. The fatigue

fracture surface for any microcrystalline ductile metal, such as an aluminium alloy, can be subdivided into three distinct zones, as shown in Fig. 22. After a crack forms, it will propagate with stage I crack growth (Fig. 22, Zone A), followed by stage II crack growth with prominent striation marks (Fig. 22, Zone B) and a final fracture (Fig. 22, Zone C) [65]. Generally, the fatigue striations of variable spacing are faintly visible in the early stage of FCG and then become clearer in the later stage [64].

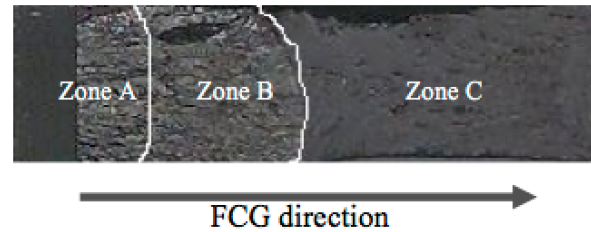


Fig. 22. Three distinct zones of FCG [67]

During the FCG process, the size of the plastic zone at the crack tip increases and encompasses several grains, thus diminishing the effect of local microstructure. As a result, the crack no longer grows along the crystallographic slip planes but instead by simultaneous or alternating shears on two slip systems [68]. The characteristic of fatigue striation is observed from the duplex slip mechanism, which produces a crack path normal to the load direction. The striations can be observed very clearly for CAL; they are well defined with regular local spacing, as shown in Fig. 23(a). However, under random loading, the striations are of unequal width and less clearly defined, as shown in Fig. 23(b).

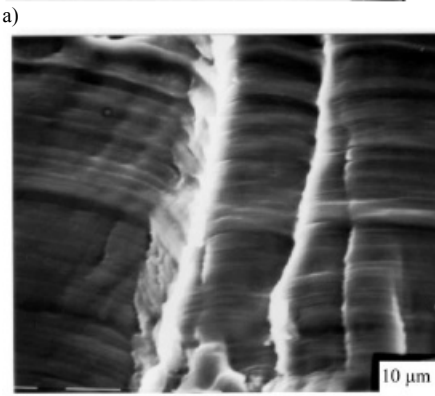
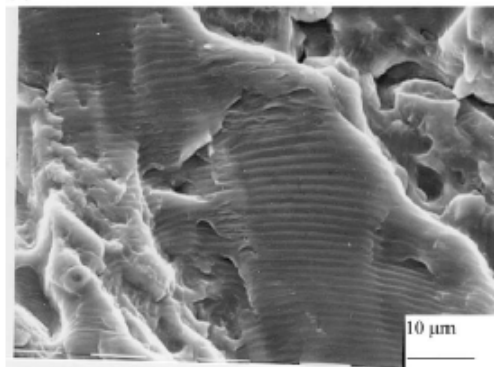


Fig. 23. Fractograph images indicate fatigue striation associated with stage II of FCG under specific loads: (a) CAL and (b) the random loading [68]

Schijve et al. [69] found other fractographic observations in their study on FCG tests under CAL and VAL loadings with a single overload and with periodic overloads/underloads. The observation of the fatigue fracture surface was performed using SEM, as shown in Fig. 24, which includes a local measurement of striation spacing. They found that local FCG rates could be determined from the measurement of the average striation spaces of a large series of striations. The measurements of the local FCG rates from striation spacing coincided with the FCG rates derived from the visual records. These findings agree with the results obtained by Jono [70], who reported that the microscopic FCG rates,  $(da/dn)_{micro}$ , could be calculated by using striation spacing, as each striation represents the applied cyclic loadings. Striation width depends on and increases with increasing stress range [71]. Striation width can also be used as an alternative method to measure the FCG rates of materials.

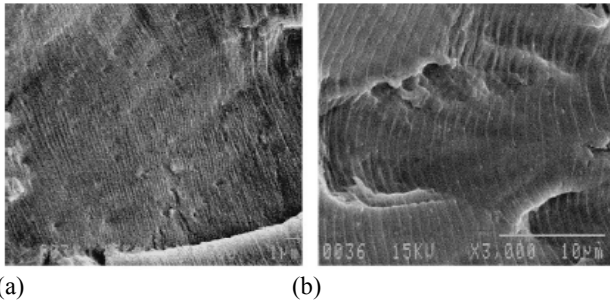


Fig. 24. A typical example of striations on fatigue fracture surface tested under two loading types: (a) CAL and (b) the periodic underloads [69]

Therefore, this review reveals that fractographic analysis is extensively used in fatigue analysis studies. Fractographic observation is important in determining the area or crack initiation to identify the direction of FCG as well as understand the material behaviour, mode of failure, and relation to failure causes. The striation mark on the fracture surface represents the characteristic of fatigue failure, and its analysis is important because it represents the applied loading conditions. Different loading sequences produce certain patterns of striation marks on the fracture surface. Moreover, the striation mark can be used to determine microscopic FCG rates if the applied loading values are known.

## 7. Conclusion and Summary

The study of the spectrum loading sequence is becoming increasingly complex because it involves loading interaction in the sequence, which depends on the combination of the overloads and/or underloads, block loading arrangement,

magnitude of load ratio, and mean stress of spectrum loading. Similarly, the sequence involves many interactions, such as that of FCG retardation and acceleration, plastic zone deformation, and crack closure effects. The magnitude of loading sequence effect is determined by many factors, such as the condition of applied loads, specimen geometry, material properties, microstructures, and the environment.

Various loading parameters and conditions that contribute to the sequence effect on fatigue life, especially at room temperature, need a more comprehensive understanding. For this reason, various configurations of cyclic loadings that precede loading sequence effects on fatigue life were reviewed and discussed. The content of this review leads to a better understanding of the loading sequence effects on the fatigue life assessment and other possible interactions.

Most studies on the effect of spectrum loading focus on the FCG rates, and only a few have been conducted on the effect on the total fatigue life, including crack initiation and propagation stages. According to the FCG findings, the knowledge of both overload and underload effects is similarly beneficial to examine. A tensile overload retards, whereas a compression underload accelerates, the FCG rates. However, the magnitude and position of overload/underload, load ratio, and mean stress in the loading sequence further influence the FCG rates. In another approach, the effects of loading sequence are presented on the fatigue fracture surface, which can be analysed by the fractographic observations. The local striation mark on the fatigue fracture surface that is subjected to VAL is slightly different from that subjected to CAL. For ductile materials such as aluminium alloy, the striation mark is clearly visible in the FCG stages and can thus be used to determine the local FCG rates.

Most research on the loading sequence effects on fatigue life assessment is conducted at room temperature. The load sequence effects, such as FCG retardation and acceleration, occur from the plastic deformation in the vicinity of the crack tip and are thus closely related to the elastic-plastic behaviour of the material. The interaction of material behaviour due to the load sequence effect with other interactions (e.g., temperature and environment) causes the higher complexity of fatigue prediction under VAL. Comprehensive knowledge on the load sequence effects and interaction at room temperature is worthy and beneficial for the further exploration of such effects in other environments because it involves further parameter interaction.

## Acknowledgement

The author would like to express gratitude to Universiti Teknikal Malaysia Melaka and Universiti Kebangsaan Malaysia for supporting this research activities.

## References

- [1] Zakaria KA, Abdullah S, Ghazali MJ, Azhari CH. Influence of spectrum loading sequences on fatigue life in a high-temperature environment. *Engineering Failure Analysis* 2013; 30: 111–123.
- [2] Zakaria KA, Abdullah S, Ghazali MJ. Elevated Temperature Fatigue Life Investigation of Aluminium Alloy Based on the Predicted S-N Curve. *Jurnal Teknologi* 2013; 63(1): 73-77.
- [3] Draper J. *Modern Metal Fatigue Analysis*. United Kingdom, Emas Publishing; 2007.
- [4] Shighley JE, Mischake CR. *Mechanical Engineering Design*. Sixth Metric Edition. New York: McGrawHill; 2003.
- [5] Post NL, Case SW, Lesko JJ. Modeling the variable amplitude fatigue of composite materials: A review and evaluation of the state of the art for spectrum loading. *International Journal of Fatigue* 2008; 30: 2064-2086.
- [6] Stephens RI, Fatemi A, Stephens RR, Fuchs HO. 2001. *Metal Fatigue in Engineering*, Second edition. New York: John Wiley & Sons; 2001.
- [7] Callister WD. *Material Science and Engineering*. New York: John Wiley & Sons; 2007.

- [8] Von V. Thermo-mechanical fatigue behaviour of the near- $\gamma$ -titanium aluminide alloy TNB-V5 under uniaxial and multiaxial loading. Thesis Doctor of Philosophy. Faculty of Mechanical Engineering, University of Bochum; 2009.
- [9] Amiri M, Khonsari MM. 2010. Rapid determination of fatigue failure based on temperature evolution: Fully reversed bending load, *International Journal of Fatigue* 2010; 32: 382-389.
- [10] Liu Y, Yu JJ, Xu Y, Sun XF, Guan HR, Hu GQ. High cycle fatigue behaviour of a single crystal super alloy at elevated temperatures. *Materials Science and Engineering A* 2007; 454-455: 357-366.
- [11] Kobayashi K, Yamaguchi K, Hayakawa M, Kimura M. Grain size effect on high-temperature fatigue properties of alloy718. *Materials Letters* 2005; 59: 383-386.
- [12] Zhu X, Shyam A, Jones JW, Mayer H, Lasecki JV, Allison JE. Effects of microstructure and temperature on fatigue behaviour of E319-T7 cast aluminium alloy in very long life cycles. *International Journal of Fatigue* 2006; 28: 1566-1571.
- [13] Rahman MM, Ariffin AK. Effects of surface finish and treatment on the fatigue behaviour of vibrating cylinder block using frequency response approach. *Journal of Zhejiang University Science A* 2006; 7(3): 352-360.
- [14] Hussain K, Wilkinson DS, Embury JD. Effect of surface finish on high temperature fatigue of a nickel based super alloy. *International Journal of Fatigue* 2009; 31: 743-750.
- [15] McKelvey SA, Fatemi A. Surface finish effect on fatigue behaviour of forged steel. *International Journal of Fatigue* 2012; 36: 130-145.
- [16] Cerny I & Mikulova D. Evaluation of overloading and crack closure effects on fatigue crack growth in an aircraft 7075-T7351 Al-alloy. *Key Engineering Materials* 2014; 577-578: 325-328.
- [17] Carvalho ALM, Martins JP, Voorwood HJC. Fatigue damage accumulation in aluminum 7050-T7451 alloy subjected to block program loading under step-down sequence. *Procedia Engineering* 2010; 2: 2037-2043.
- [18] Lee SY, Liaw PK, Choo H, Rogge RB. A study on fatigue crack growth behaviour subjected to a single tensile overload: Part I. An overload-induced transient crack growth micromechanism. *Acta Materialia* 2011; 59: 485-494.
- [19] Daneshpour S, Dyck J, Ventzke V, Huber N. Crack retardation mechanism due to overload in base material and laser welds of Al alloy. *International Journal of Fatigue* 2012; 42: 95-103.
- [20] Burns JT, Kim S, Gangloff RP. Effect of corrosion severity on fatigue evolution in Al-Zn-Mg-Cu. *Corrosion Science* 2010; 52: 498-508.
- [21] Uematsu Y, Akita M, Nakajima M, Tokaji K. Effect of temperature on high cycle fatigue behaviour in 18Cr-2Mo ferritic stainless steel. *International Journal of Fatigue* 2007; 30: 642-648.
- [22] Daoud A, Vogta JB, Charkaluk E, Zhang L, Biasci JC. Effect of temperature on the low cycle fatigue behavior of Glidcop Al-15. *Procedia Engineering* 2010; 2: 1487-1495.
- [23] Tomioka JI, Kiguchi K, Tamura Y, Mitsuishi H. Influence of temperature on the fatigue strength of compressed-hydrogen tanks for vehicles. *International Journal of Hydrogen Energy* 2011; 36: 2513-2519.
- [24] Giglio M, Manes A. Crack propagation on helicopter panel: Experimental test and analysis. *Engineering Fracture Mechanics* 2007; 75: 866-879.
- [25] Lee YL, Pan J, Hathaway RB, Barkey ME. Fatigue testing and analysis (Theory and Practice). USA: Elsevier Butterworth-Heinemann; 2005.
- [26] Rahman MM, Ariffin AK, Jamaludin N, Haron CHC. Fatigue behaviour of 6000 series aluminum alloys on cylinder block of free piston linear engine using total life approach. *Jurnal Mekanikal* 2006; 21: 1-15.
- [27] Rice RC, Jackson JL, Bakuckas J, Thompson S. Metallic materials properties development and standardization. Scientific Report, Department of Transportation, Federal Aviation Administration. Washington DC; 2003.
- [28] Kihl DP, Sarkani S. Mean stress effects in fatigue of welded steel joints. *Probabilistic Engineering Mechanics* 1999; 14: 97-104
- [29] Mann T. The influence of mean stress on fatigue crack propagation in aluminium alloys. *International Journal of Fatigue* 2007; 29: 1393-1401.
- [30] Abdullah S, Nizwan CKE, Nuawi MZ. A study on fatigue data editing using the Short-Time Fourier Transform (STFT). *American Journal of Applied Sciences* 2009; 6: 565-575.
- [31] Ribeiro AS and de Jesus MP. Fatigue behaviour of welded joints made of 6061-T651 aluminium alloy, in: *Aluminium Alloy, Theory and Application*, edited by T.Kvackaj, InTech Publishing; 2011.
- [32] Kadhim NA, Abdullah S, Ariffin AK. Effect of fatigue data editing technique associated with finite element analysis on the computer fatigue design period. *Materials and Design* 2011; 32: 1020-1030.
- [33] Xiong JJ, Sheno RA. A load history generation approach for full-scale accelerated fatigue tests. *Engineering Fracture Mechanics* 75; 2008: 3226-3243.
- [34] Ngiau C, Kujawski D. Sequence effects of small amplitude cycles on fatigue crack initiation and propagation in 2024-T351 aluminium. *International Journal of Fatigue* 2001; 23: 807-815.
- [35] Pereira HFSG, de Jesus AMP, Ribeiro AS, Fernandes AA. Influences of loading sequence and stress ratio on fatigue damage accumulation of a structural component, *Science and Technology of Materials* 2008; 20: 60-67.
- [36] Jassen M, Zuidema J, Wanhill R. *Fracture Mechanics*. Second edition. London: Spon Press; 2004.
- [37] Beden SM, Abdullah S, Ariffin AK, Al-Asady NA. Fatigue crack growth simulation of aluminium alloy under spectrum loading. *Materials and Design*. 2010; 31(7): 3449-3456.
- [38] Ray A, Patankar R. Fatigue crack growth under variable-amplitude loading: Part I, Model formulation in-state space setting. *Applied Mathematical Modelling* 2001; 25: 979-994.
- [39] Borrego LP, Costa JM, Ferreira JM. Fatigue crack growth in thin aluminium alloy sheet under loading sequences with periodic overloads. *Thin-Walled Structures* 2005; 43: 772-788.
- [40] Zitounis V, Irving PE. Fatigue crack acceleration effects during tensile underloads in 7010 and 8090 aluminium alloys. *International Journal of Fatigue* 2007; 29: 108-118.
- [41] Mikheevskiy S, Glinka G. Elastic-plastic fatigue crack growth analysis under variable amplitude loading spectra. *International Journal of Fatigue* 2009; 31: 1828-1836.
- [42] Pommier S. Cyclic plasticity and variable amplitude fatigue. *International Journal of Fatigue* 2003; 25: 983-997.
- [43] Daneshpour S, Koçak M, Langlade S, Horstmann M. Effect of overload on fatigue crack retardation of aerospace Al-alloy laser welds using crack-tip plasticity analysis. *International Journal of Fatigue* 2009; 31: 1603-1612.
- [44] Taheri F, Trask D, Pegg N. Experimental and analytical investigation of fatigue characteristics of 350WT steel under constant and variable amplitude loadings. *Journal of Marine Structure* 2003; 16: 69-91.
- [45] Ray S, Kishen JMS. Fatigue crack growth due to overloads in plain concrete using scaling laws. *Sadhana* 2012; 37(1): 107-124.
- [46] Ishihara S, McEvily AJ, Goshima T, Nishino S, Sato M. The effect of the R value on the number of delay cycles following an overload. *International Journal of Fatigue* 2008; 30: 1737-174.
- [47] Harmain GA. A model for predicting the retardation effect following a single overload. *Theoretical and Applied Fracture Mechanics* 2010; 53: 80-88.
- [48] Huang XP, Zhang JB, Cui WC, Leng JX. Fatigue crack growth with overload under spectrum loading. *Theoretical and Applied Fracture Mechanics* 2005; 44: 105-115.
- [49] Fang QZ, Wang TJ, Li HM. Overload effect on the fatigue crack propagation of PC/ABS alloy. *Polymer* 2007; 48: 6691-6706.
- [50] Tur YK, Vardar O. Periodic tensile overloads in 2024-T3 Al-alloy. *Engineering Fracture Mechanics* 1996; 53(1): 69-77.
- [51] Hammouda MMI, Ahmad SSE, Seleem MH, Sallam HEM. Fatigue crack growth due to two successive single overloads. *Fatigue & Fracture of Engineering Materials Structures* 1998; 21: 1537-47.
- [52] Lang M, Marci G. The influence of single and multiple overloads on fatigue crack propagation. *Fatigue & Fracture of Engineering Materials & Structures* 1999; 22: 257-71.
- [53] Varvani-Farahani A, Sharma M, Kianoush MR. Fatigue damage analysis and life assessment under variable amplitude loading conditions. *Materials Science and Engineering A* 2005; 403: 42-47.
- [54] Silva FS. Fatigue crack propagation after overloading and underloading at negative stress ratios. *International Journal of Fatigue* 2007; 29: 1757-1771.
- [55] Olagnon M, Guede Z. Rainflow fatigue analysis for loads with multimodal power spectral density. *Marine Structures* 2008; 21: 160-176.
- [56] Liu Y, Mahadevan S. Stochastic fatigue damage modeling under variable amplitude loading. *International Journal of Fatigue* 2007; 29: 1149-1161.
- [57] Robert M, Engle JR. Damage accumulation techniques in damage tolerance analysis in: *Damage Tolerance in Metallic Structures*. Edited by Chang and Rudd. Ann Arbor: American Society for Testing and Material; 1984.

- [58] Abdullah S, Choi JC, Giacomini JR, Yates JR. Bump extraction algorithm for variable amplitude fatigue loading. *International Journal of Fatigue* 2006; 28: 675-691.
- [59] Lin CK, Teng HY. Creep properties of Sn-3.5Ag-0.5Cu lead-free solder under step-loading. *Journal of Materials Science: Mater Electron* 2006; 13: 577-586.
- [60] Walter M, Aktaa J, Lerch M. Failure behaviour of EUROFER 97 in the low-cycle fatigue region under multi-step loading. *International Journal of Fatigue* 2008; 30: 568-573.
- [61] Borrego LP, Ferreira JM, Costa JM. Partial crack closure under block loading. *International Journal of Fatigue* 2008; 30: 1787-1796.
- [62] Kihl DP, Sarkani S. Mean stress effects in fatigue of welded steel joints *Probabilistic Engineering Mechanics* 1999; 14: 97-104.
- [63] Chu CC, Chernenkoff RA. Crack closure-based analysis of fatigue tests with mean stresses. *International Journal of Fatigue* 2001; 23: S187-S194.
- [64] Lee EU, Glinka G, Vasudevan AK, Iyyer N, Phan ND. Fatigue of 7075-T651 aluminium alloy under constant and variable amplitude. *International Journal of Fatigue* 2009; 31:1858-1864.
- [65] De PS, Mishra RS and Smith CB. Effect of microstructure on fatigue life and morphology in an aluminum alloy. *Scripta Materiala* 2008; 60: 500-503.
- [66] Begum S, Chen DL, Xu S, Luo AA. Low cycle fatigue properties of an extruded AZ31 magnesium alloy. *International Journal of Fatigue* 2009; 31:726-735.
- [67] Zakaria KA, Abdullah S, Ghazali MJ, Nopiah ZM. Fractography analysis of Al6061 under fatigue spectrum loadings. *Engineering e-Transaction* 2012; 7(1): 28-33.
- [68] Wei LW, de los Rios ER, James MN. Experimental study and modelling of short fatigue crack growth in aluminium alloy A17010-T7451 under random loading. *International Journal of Fatigue* 2002; 24: 963-975.
- [69] Schijve J, Skorupa M, Skorupa A, Machniewicz T, Gruszczynski P. Fatigue crack growth in the aluminium alloy D16 under constant and variable amplitude loading. *International Journal of Fatigue* 2004; 26: 1-15.
- [70] Jono M. Fatigue damage and crack growth under variable amplitude loading with reference to the counting methods of stress-strain ranges. *International Journal of Fatigue* 2005; 27:1006-1015.
- [71] Callister WD. *Material Science and Engineering*. New York: John Wiley & Sons; 2007.